Pyrolytic carbon surfaces investigated by atomic force microscopy

Andreas Pfrang[1,*], Thomas Schimmel[1, 2]
[1] Institute of Applied Physics, University of Karlsruhe, D-76128 Karlsruhe, Germany
[2] Institute of Nanotechnology, Forschungszentrum Karlsruhe, D-76021 Karlsruhe, Germany
Email: info@pyrocarbon.de

Keywords
Pyrolytic carbon, atomic force microscopy, nucleation

INTRODUCTION

The evolution of the micro- and nanostructure of pyrolytic carbon determines the properties of the resulting pyrocarbon layers. This evolution starts with the nucleation of carbon islands on the substrate material and ends with the formation of the surface of the pyrolytic carbon layer.
Here, both situations were investigated by atomic force microscopy on native pyrolytic carbon surfaces. Nucleation mechanisms were investigated by studying the initial stages of pyrolytic carbon deposition. Additionally, complete pyrolytic carbon film surfaces were investigated by AFM. The resulting AFM topography images were evaluated to obtain statistical data on the size distributions of pyrolytic carbon islands.

EXPERIMENTAL

Sample preparation

Pyrolytic carbon was deposited in a hot-wall reactor at 1100°C on different substrates at residence times up to 4 s. Deposition times between 5 minutes and a few 100 h were chosen. Methane / argon mixtures or pure methane at total pressures up to 100 kPa were used. The native pyrolytic carbon surfaces were investigated by atomic force microscopy.

Atomic Force Microscopy

Atomic force microscopy (AFM) was performed with a homebuilt AFM equipped with commercial control electronics (Universal Controller, Park Scientific Instruments) at ambient conditions. Commercially available V-shaped silicon and silicon nitride cantilevers were used. The images were taken in the contact mode of the AFM.

RESULTS AND DISCUSSION

The island size distribution was determined based on AFM topography data using different methods: One method is the manual measurement of the diameter of each island on the AFM images. This method is obviously time consuming and leads to a strong influence of the subjective definition of an island.

* Author to whom any correspondence should be addressed.

A second possibility is the detection of islands with a software code followed by an automated evaluation of the island diameters. In this case a reproducible result is obtained, but the algorithms do not identify all the islands that would be identified on the AFM images with the eye or islands are detected that one would not call islands by judging with the eye. Here, the AnalySIS software (Soft Imaging System, Münster, Germany) was used (Pfrang, 2005).

Both methods are compared for the example given in Fig. 1. The AFM topography image is shown top left. The top right image shows the island boundaries detected by the software overlaid to the topography image. In principle the software allows to adjust the island boundaries by hand, but this has not been done to eliminate subjective influences.

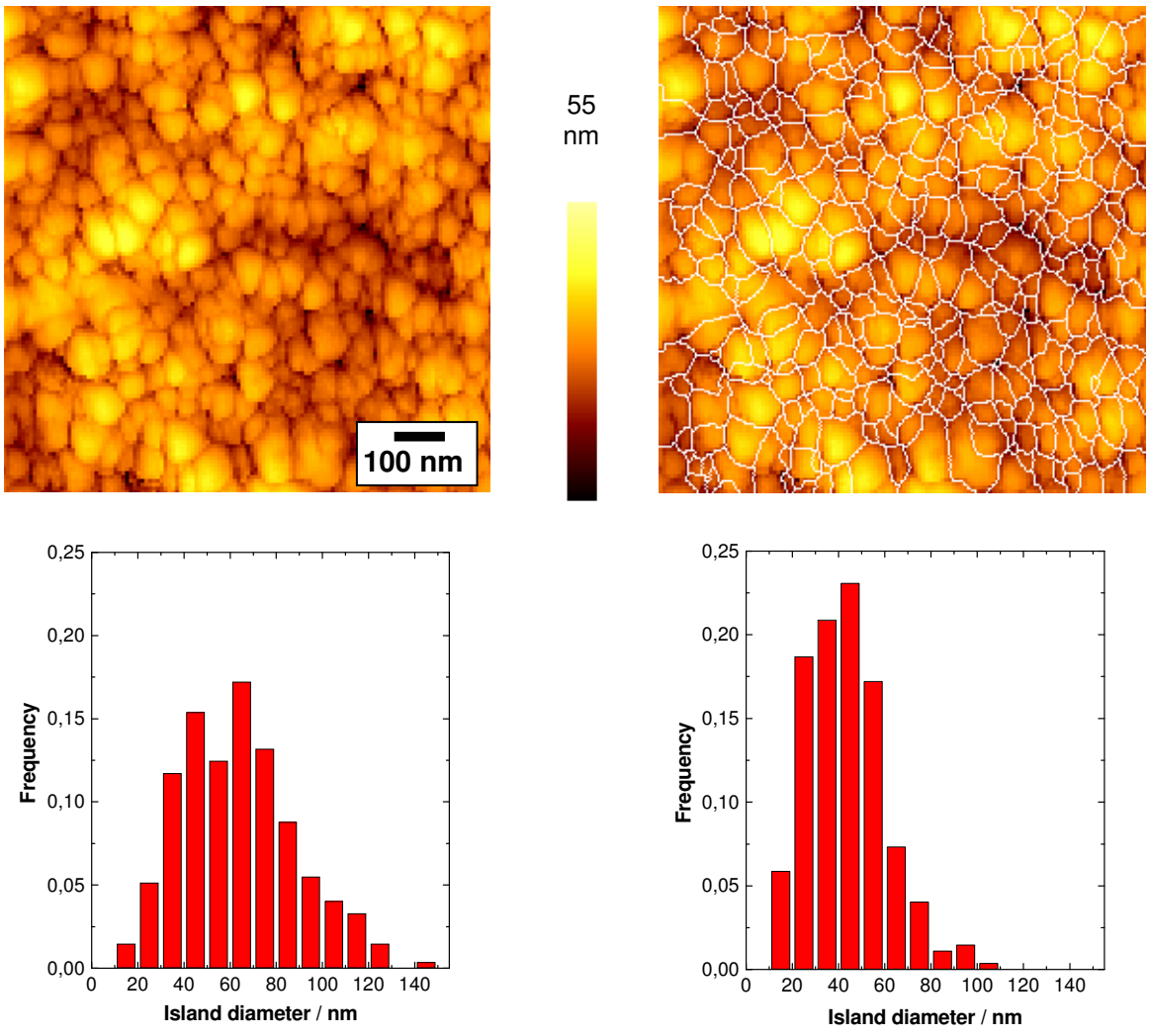

FIGURE 1: Determination of the island size distribution. The top left image shows an AFM topography image of a pyrolytic carbon layer deposited on pyrolytic boron nitride. Deposition parameters: $p_{methane}$ 10 kPa, p_{argon} 80 kPa, deposition time 50 h, residence time 0.6 s. The boundaries between islands were determined automatically using the AnalySIS Software (Soft Imaging System, Münster, Germany), see top right. The resulting island diameter distribution is shown in the bottom left image. The bottom right image shows the island diameter distribution determined by measuring the diameters of the islands by hand for the same AFM topography image (top left) for comparison.

The bottom images of Fig. 1 show the distribution of the island diameters determined automatically by the software (left) in comparison with the distribution acquired manually (right). Islands at the edges of the topography images were not taken into account for both methods.

The methods do not only give different island size distributions but also different average diameters: 63.8 nm for the software evaluation as compared to 43.2 nm for manual evaluation. Also the island area is smaller for manual evaluation (1698 nm^2) as compared to software evaluation (2345 nm^2).
For the software evaluation, the whole image area is covered by islands, whereas the lower overall island area determined manually indicates that for manual evaluation not the whole topography image is considered as covered with islands.

The statistical data of island sizes presented in the following were determined by software evaluation. Table 1 summarizes the deposition parameters of the evaluated samples.

Sample name	Substrate	$p_{methane}$	p_{argon}	Residence time at the end τ	Deposition time t
Si 20	Silicon	9.8 kPa	90 kPa	2.0 s	60 min
		0.2 kPa O_2			
Si 22	Silicon	10 kPa	90 kPa	2.0 s	60 min
P 15	Silicon	10 kPa	90 kPa	2.0 s	90 min
P 23	Silicon	10 kPa	90 kPa	2.0 s	90 min
PyroSi 0.6 s	Silicon	10 kPa	91 kPa	0.6 s	6 h
PyroSi 2.4 s	Silicon	10 kPa	91 kPa	2.4 s	6 h
PyroBN 1s	Boron nitride	10 kPa	80 kPa	1.0 s	50 h
PyroBN 4s	Boron nitride	10 kPa	80 kPa	4.0 s	50 h
PyroSG	Sigradur	10 kPa	90 kPa	1.0 s	9.5 h
Coated C-fiber	C-fiber	20 kPa	0 kPa	0.5 s	120 min
Cordierite S25	Cordierite	4 kPa	0 kPa	1.0 s	185 h

TABLE 1: Deposition parameters of the evaluated samples. The deposition was carried out in a hot wall reactor at a temperature of 1100°C.

Table 2 summarizes the statistical data of the island size distribution. AFM topography images of two different sizes were evaluated: 1 µm x 1 µm (first value in each cell) and 2 µm x 2 µm (second value). In almost all cases the average island size is larger for the image with the larger scan area. This is not surprising as for larger topography images smaller islands can not be detected within the resolution of the AFM images any more.

The distributions of the island diameters were fitted with Gaussian profiles. The maximum of the Gaussian fit function as well as the standard deviation of this function are given in Table 2. The peak positions of the Gaussian fit functions are almost always smaller than the average diameters. This indicates that the distribution of the island diameters is not a Gaussian function.

Sample	Residence time	Average area / 10^3 nm^2	Standard deviation area / 10^3 nm^2	Average diameter / nm	Standard deviation diameter / nm	Peak of Gauss fit / nm	Standard deviation Gauss fit/ nm
Si 20	0.25 s	6.2 / 8.2	4.3 / 5.9	104 / 118	37 / 43	96 / 111	37 / 42
	0.75 s	5.2 / 9.5	4.5 / 6.6	93 / 128	40 / 48	83 / 122	36 / 50
	1.25 s	6.3 / 7.5	4.2 / 6.2	106 / 111	37 / 48	102 / 101	41 / 46
	1.75 s	6.9 / 9.8	3.7 / 7.4	112 / 131	37 / 51	103 / 120	46 / 50
Si 22	0.75 s	4.0 / 6.1	3.2 / 4.8	83 / 99	33 / 39	76 / 93	32 / 37
	1.75 s	4.4 / 7.6	3.8 / 6.7	71 / 78	40 / 53	80 / 100	43 / 57
P15	1.14 s	5.2 / 10	2.2 / 3.7	95 / 136	**22 /** 27	85 / 125	**22 /** 27
	1.35 s	10 / 14	3.8 / 12	136 / 153	36 / 41	115 / 135	30 / 32
	1.56 s	- / 12	- / 4.9	- / 147	- / 31	- / 131	- / 29
	1.77 s	27 / 26	11 / 10	223 / 215	58 / 51	195 / 185	41 / 40
	2.18 s	24 / 32	7.7 / 11	225 / 254	52 / 56	205 / 232	29 / 51
P23	1.55 s	11 / 10	4.2 / 3.9	141 / 130	33 / 26	127 / 118	29 / 27
	2.17 s	- / **61**	- / **22**	- / **346**	- / 47	- / **304**	- / 42
PyroSi 0.6s	0.3 s	5.1 / 14	5.6 /13	92 / 156	55 / **72**	71 / 140	49 / **70**
PyroSi 2.4s	1.2 s	7.9 / -	9.3 / -	110 / -	64 / -	87 / -	52 / -
PyroBN 1s	0.17 s	4.3 / 11	3.9 / 7.7	87 / 132	40 / 48	79 / 111	38 / 51
	0.5 s	2.9 / 3.6	2.2 / 2.9	71 / 78	29 / 32	67 / 69	31 / 29
	0.83 s	6.0 / -	5.2 / -	99 / -	44 / -	91 / -	42 / -
PyroBN 4s	0.67 s	4.3 / 6.0	3.5 / 4.8	85 / 100	35 / 42	80 / 91	36 / 37
	2.0 s	**2.5 /** 2.6	**2.1 /** 2.2	**64 / 64**	28 / 29	60 **/ 57**	28 / 29
PyroSG	0.17 s	2.6 / -	**2.1 /** -	66 / -	28 / -	61 / -	29 / -
Coated C-fiber	0.5 s	5.4 / -	4.9 / -	111 / -	52 / -	96 / -	39 / -
Cordierite S25	0.125 s	5.1 / 5.7	4.0 / 4.6	93 / 97	38 / 43	85 / 88	32 / 40

TABLE 2: Statistical data for island areas and island diameters determined by software analysis of AFM topography images of different pyrolytic carbon films. The first value was determined from topography images with a size of 1 µm x 1 µm, the second value from images with a size of 2 µm x 2 µm. The minimum and maximum of each column are written in bold letters. Peak of Gauss fit gives the value where the Gauss fit of the distribution of diameters has the maximum value.

The investigated samples do not cover the whole range of possible pyrolytic carbon layers, but typical parameters can be deduced: the average island diameters are in the range between 64 nm and 346 nm. A typical average diameter is about 100 nm. Large deviations from this value (> 50 %) are only rarely found. It should be noted that an increase of the island diameter with increasing degree of texture was reported recently for pyrolytic carbon deposited in a hot wall reactor (De Pauw, 2006).

AFM allows the identification of separate pyrolytic carbon islands that are deposited in the initial stages of pyrolytic carbon deposition by chemical contrast imaging (Müller, 2005;

Pfrang, 2004). This method is used here to investigate the nucleation mechanisms for the deposition of pyrolytic carbon.

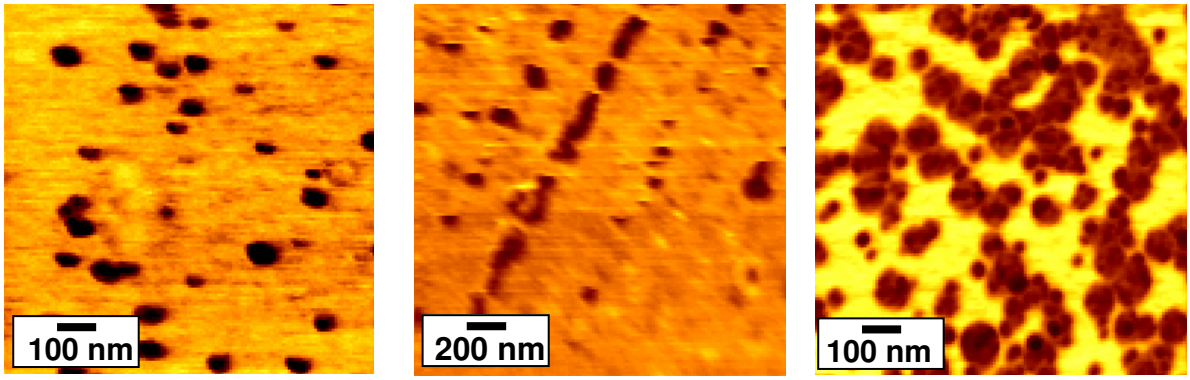

FIGURE 2: Chemical contrast images of pyrolytic carbon islands (dark) deposited on silicon substrates. Left image: **Random nucleation**, $p_{methane}$ 20 kPa, p_{argon} 80 kPa, deposition time 5 min, residence time 1.06 s, Center image: **Line nucleation**, $p_{methane}$ 10 kPa, p_{argon} 90 kPa, deposition time 90 min, residence time 0.05 s, Right image: **Secondary nucleation**, $p_{methane}$ 20 kPa, p_{argon} 80 kPa, deposition time 5 min, residence time 1.33 s. Reactor temperature 1100°C for all three samples.

Fig. 2 shows three different nucleation mechanisms:

- Randomly distributed nucleation of separate islands on the substrate surface, where point like defects, if available, might act as nucleation centers (left image).
- Nucleation along line-shaped defects on the substrates like fine scratches or creases (center image).
- Preferred nucleation of new islands at the edges of already existing islands, which will be denoted as secondary nucleation in the following (right image).

During the transition from separate islands to a closed layer, it has been found that with increasing carbon coverage the average island diameter increases up to a certain value and is then constant (Pfrang, 2004).

CONCLUSIONS

Atomic force microscopy was applied to study the micro- and nanostructure of native pyrolytic carbon surfaces. All surfaces of complete layers exhibited a granular surface structure. It was found that the method for the evaluation of the island size distribution influences the results. Software evaluation showed that the typical average island diameter was 100 nm and deviations larger than 50 % from this value were only rarely observed. Minimum and maximum average grain sizes were 64 nm and 346 nm, respectively.
For the initial stages of pyrolytic carbon deposition, three nucleation mechanisms were observed: random nucleation, nucleation along lines and the preferred nucleation at the edges of already existing islands.

Acknowledgements
The authors thank W. Send and K.J. Hüttinger for sample synthesis and fruitful discussions and the Deutsche Forschungsgemeinschaft for financial support within the Collaborative Research Center (SFB) 551.

References

De Pauw V., Collin A., Send W., Hawecker J., Gerthsen D., Pfrang A., Schimmel Th. (2006). Deposition rates during the early stages of pyrolytic carbon deposition in a hot-wall reactor and the development of texture. *Carbon*, 44, in press.

Müller M. (2005). Kraftmodulationsmikroskopie: Detektionsverhalten – Kontrastmechanismus – Anwendungen. PhD thesis, University of Karlsruhe, Cuvillier Verlag, Göttingen, Germany, ISBN 3-86537-341-0.

Pfrang A., Wan Y. Z., De Pauw V., Send W., Gerthsen D., Schimmel Th. (2004). Early stages of the chemical vapor deposition of pyrolytic carbon investigated by atomic force microscopy. Proceedings of Carbon 2004, Providence, USA.

Pfrang A. (2005). Von den Frühstadien der Pyrokohlenstoffabscheidung bis zum Kompositwerkstoff - Untersuchungen mit Rastersondenverfahren. PhD thesis, University of Karlsruhe, Verlag Dr. Hut, München, Germany, ISBN 3-89963-133-1.